

Phenomenology of Diffractive DIS

Nikolai N. Nikolaev^{a),b),c)} and Bronislav G.Zakharov^{c)}

^{a)}ITKP der Universität Bonn, Nussallee 14-16, D-53115 Bonn

^{b)}IKP, KFA Jülich, D-52425 Jülich, Germany

^{c)}L.D.Landau Institute, Kosygina 2, 1117 334 Moscow, Russia

Abstract. The recent progress in the QCD theory of diffractive DIS (DDIS) is reviewed. We place emphasis on pQCD scales, diffractive factorization breaking, jet and charm production and new fundamental observables which are becoming accessible with the Leading Proton Spectrometers (LPS) of ZEUS and H1.

DIFFRACTIVE STRUCTURE FUNCTIONS

This is an opening talk on diffraction at DIS'97 and we start with definitions. The longitudinal (L) and the two transverse (T) polarizations of the exchanged photon define the four components $d\sigma_i^{(3)}(\gamma^*p \rightarrow p'X)/dM^2 dp_\perp^2 d\phi$ ($i = T, L, TT'$ and LT') in the expansion

$$Q^2 x \frac{d\sigma^{(5)}(ep \rightarrow e'p'X)}{dQ^2 dx dM^2 dp_\perp^2 d\phi} = \frac{\alpha_{em}}{\pi} \left\{ (1-y + \frac{1}{2}y^2) \cdot d\sigma_T^{D(3)} + (1-y) \cdot d\sigma_L^{(3)} \right. \\ \left. + (1-y) \cos 2\phi \cdot d\sigma_{TT'}^{D(3)} + (2-y) \sqrt{1-y} \cos \phi \cdot d\sigma_{LT'}^{D(3)} \right\} / dM^2 dp_\perp^2 d\phi \quad (1)$$

where M is the diffractive mass, \vec{p}_\perp is the (p, p') momentum transfer, and ϕ is the angle between the (e, e') and (p, p') planes. In the charged current (CC) DDIS there are also the C- and P-odd, TT' and LT' , terms [1]. Each $d\sigma_i^{(3)}$ defines a set of **dimensionless** diffractive structure functions $F_i^{D(5)}$,

$$\frac{2\pi(Q^2 + M^2)d\sigma_i^{(3)}(\gamma^*p \rightarrow p'X)}{dM^2 dp_\perp^2 d\phi} = \frac{\sigma_{tot}^{pp}}{16\pi} \cdot \frac{4\pi^2 \alpha_{em}}{Q^2} \cdot F_i^{D(5)}(\phi, p_\perp^2, x_{\mathbf{P}}, \beta, Q^2), \quad (2)$$

$F_i^{D(4)}(p_\perp^2, x_{\mathbf{P}}, \beta, Q^2) = \int \frac{d\phi}{2\pi} F_i^{D(5)}$ and $F_i^{D(3)}(x_{\mathbf{P}}, \beta, Q^2) = \frac{\sigma_{tot}^{pp}}{16\pi} \int dp_\perp^2 F_i^{D(4)}$. The so-defined $F_i^{D(3)}$ are smooth functions of $x_{\mathbf{P}}, \beta, Q^2$, in contrast to the ZEUS/H1 definition of $F_2^{D(3)}$ [2] which blows up at $x_{\mathbf{P}} \rightarrow 0$ due to the extra factor $1/x_{\mathbf{P}}$. Here $\beta = Q^2/(Q^2 + M^2)$ and $x_{\mathbf{P}} = x/\beta$ are the DDIS variables.

The microscopic QCD mechanism of DDIS, as developed in 1991 by Nikolaev and Zakharov [3–5], is a grazing, quasielastic scattering of multiparton Fock states of the γ^* on the proton. DDIS is best described viewing γ^* as a system of color dipoles spanning between quarks, antiquarks and gluons [3–5], interaction of which with the target proton is described by the color dipole cross section $\sigma(x, r) = \frac{\pi^2}{3} r^2 \alpha_S(r) G(x, q^2 \approx 10/r^2)$ [6]. Here $G(x, q^2)$ is the gluon structure function of the target nucleon and one sums the Leading $\text{Log}_x^{\frac{1}{2}}$ pQCD diagrams for the color singlet two-gluon exchange. Systematic expansion of DDIS in excitations of the $q\bar{q}, q\bar{q}g$ and higher Fock states of the photon has been developed in [4,5,7–11]. The technique [4,5,7] has been a basis of all the subsequent pQCD works on DDIS [12]. The Buchmuller et al. model [13] is essentially identical to the color dipole picture; their function $W(r)$ is an exact counterpart of our $\sigma(x, r)$ evaluated in the pQCD Born approximation. Bjorken’s aligned jet model [14] is an integral part of the color dipole approach. For the 1996 status report at DIS’96 see [15].

This extended presentation reviews also the new results reported at DIS’97.

DIPOLE SIZES AND PQCD SCALES IN DDIS

Vector meson production $\gamma^* p \rightarrow V p$ is an exclusive DDIS. For the shrinkage of γ^* the typical dipole size (the scanning radius) contributing to the production amplitude equals $r_S = 6/\sqrt{Q^2 + m_V^2}$ and one finds [17,18]:

$$\sigma_L \propto Q^2 r_S^2 \sigma^2(x_{\mathbf{P}}, r_S) \propto G^2(x_{\mathbf{P}}, q_L^2) Q^2 / (Q^2 + m_V^2)^4. \quad (3)$$

For the factor 6 in r_S the relevant pQCD scale, $q_{T,L}^2 = \tau_{T,L}(m_V^2 + Q^2)$, is rather small: $\tau_L = 0.1-0.2$ and $\tau_T = 0.07-0.15$ [19]. Eq. (3) is a basis of the very successful pQCD phenomenology of vector meson production ([19–21] and references therein). The exponent Δ_{eff} in $\sigma_L \sim (W^2)^{2\Delta_{eff}}$, rises with Q^2 due to the rise of the pQCD scales $q_{L,T}^2$, in good agreement with the experiment.

DDIS into continuum at $\beta \gtrsim 0.1-0.2$ is dominated by the $q\bar{q}$ excitation. If \vec{k} is the transverse momentum of the q jet w.r.t. the photon, then [4,7,10,11]

$$\begin{aligned} \frac{dF_T^{D(3)}}{dk^2} &\sim \left(1 - \frac{2(k^2 + m_f^2)}{M^2}\right) \cdot \frac{1}{(k^2 + m_f^2)^2} \cdot G^2(x_{\mathbf{P}}, q_T^2 = \frac{m_f^2 + k^2}{(1-\beta)}), \\ \frac{dF_L^{D(3)}}{dk^2} &\sim \frac{1}{Q^2} \cdot \frac{1}{(k^2 + m_f^2)} \cdot G^2(x_{\mathbf{P}}, q_L^2 = \frac{m_f^2 + k^2}{(1-\beta)}). \end{aligned} \quad (4)$$

These results have been re-derived by several groups [12]. Because $q_{T,L}^2 \propto k^2$, we predict strong enhancement of large- k jets. Furthermore, $F_L^{D(3)}$ is dominated by hard jets and scaling violations almost entirely compensate the higher twist behavior of $F_L^{D(3)} \propto \frac{1}{Q^2} \beta^3 (1-2\beta)^2 G^2(x_{\mathbf{P}}, \frac{1}{4\beta} Q^2)$ [11] which, for $\beta \gtrsim 0.9$, completely takes over the leading twist transverse structure function [4,10], $F_T^{D(3)} \propto \frac{1}{m_f^2} \beta (1 -$

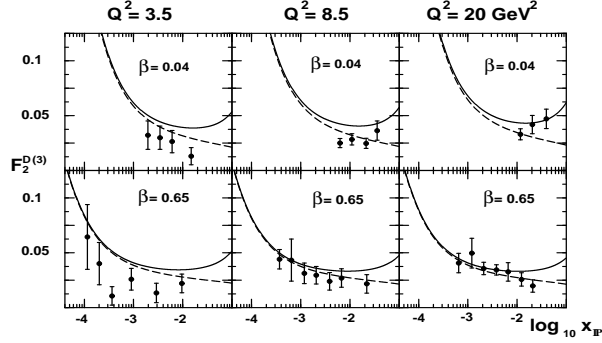


FIGURE 1. The dashed curve is the 1994 predictions for $F_2^{D(3)}$ from the color dipole model [8], the solid curve includes the f -reggeon and pion exchange evaluated in [24], the experimental data are from H1 [25].

$\beta)^2(3 + 4\beta + 8\beta^2)G^2(x_{\mathbf{IP}}, q_T^2 \approx \frac{m_V^2}{(1-\beta)})$. The applicability of pQCD improves for large β . One often fits $F_2^{D(3)} \propto x_{\mathbf{IP}}^{2(1-\alpha_{\mathbf{IP}})}$. The rise of our fixed- M pQCD scale $q_T^2 \sim \frac{1}{4}m_V^2(1 + \frac{Q^2}{M^2})$ predicts the rise of $\alpha_{\mathbf{IP}}$ with Q^2 . Furthermore, at $Q^2 \gtrsim 10M^2$ one enters the F_L^D dominated region of $q_L^2 \sim \frac{1}{4}Q^2$ and $\alpha_{\mathbf{IP}}$ must become as large as for vector meson production, which is indeed seen in the fixed- M data from ZEUS [22]. This is one of the manifestations of the duality between the continuum and vector meson production derived in [11]. For fixed β , the exponent $\alpha_{\mathbf{IP}}$ must not depend on Q^2 .

Production of $q\bar{q}$ dijets in DDIS at $\beta \ll 1$, and/or by real photons, is especially interesting. In 1994 we showed that in this case the transverse momentum k of jets probes directly the transverse momentum of gluons in the pomeron [7] and $d\sigma_T^D \propto |\partial G(x_{\mathbf{IP}}, k^2)/\partial \log k^2|^2$.

DDIS at $\beta \lesssim 0.1-0.2$ comes from excitation of the $q\bar{q}g$ and higher Fock states of the photon. It is DIS off the pomeron sea with the typical sea structure function, $F_T^{D(3)}(x_{\mathbf{IP}}, \beta, Q^2) \sim G^2(x_{\mathbf{IP}}, q_{sea}^2 \approx \mu_G^2)$, which obeys an approximate triple-pomeron factorization conjectured in [3,4] and derived in [5,9],

$$F_2^{D(4)}(p_{\perp}^2 = 0, x_{\mathbf{IP}}, \beta, Q^2) \approx \frac{16\pi A_{3\mathbf{IP}}}{\sigma_{tot}^{pp}} F_{2p}(x_{\mathbf{IP}}, q_{sea}^2), \quad (5)$$

which is similar to the triple-pomeron limit of soft diffraction ($a = p, \pi, K, \gamma$) $M^2 d\sigma(ap \rightarrow p'X)/dp_{\perp}^2 dM^2|_{p_{\perp}^2=0} = A_{3\mathbf{IP}} \sigma_{tot}^{ap} \cdot$. Here $R_c = 1/\mu_G \sim 0.2-0.3 fm$ is a propagation radius for perturbative gluons. In [9] we showed that although $A_{3\mathbf{IP}} \approx 0.15-0.2 \text{ GeV}^{-2}$ is the dimensional quantity, it does not change much from $Q^2 = 0$ to DIS; parametrically $A_{3\mathbf{IP}} \propto R_c^2$. The normalization of the pomeron sea structure function **predicted** in [4,8] is in good agreement with the experiment, see [2] and Fig. 1.

CC DDIS has several peculiarities [1]: First, both the $F_T^D(3)$ and $F_L^D(3)$ receive extra contributions, and $F_L^D(3)$ is anomalously large at small Q^2 because of the

nonconservation of weak currents, for the similar findings in standard DIS see [23]. Second, in the large- β CC DDIS with e^+ beams one excites the $c\bar{s}$ pairs and the pQCD scale q_T^2 is different for DDIS with leading charm, $q_T^2 \sim m_s^2/(1-\beta)$ and leading (anti)strangeness, $q_T^2 \sim m_c^2/(1-\beta)$. Third, the k^2 distribution of the charm changes from the forward to backward hemispheres in the diffractive system.

DIFFRACTIVE FACTORIZATION, QCD EVOLUTION AND HIGHER TWISTS

The interpretation of $q\bar{q}$ excitation as DIS off the intrinsic $q\bar{q}$ of the pomeron must be taken with the grain of salt, because for the above variety of pQCD scales $(\mu_G^2, m_f^2, \frac{1}{4}Q^2)$, the flavor, valence, sea and glue composition of the pomeron changes with $x_{\mathbf{P}}$ [8]. Furthermore, because the pQCD scales $q_{T,L}^2$ depend on β , and the $x_{\mathbf{P}}$ and β dependences are inextricably entangled, it is crystal clear that the often postulated [26], but never proven, diffractive and/or Ingelman-Schlein factorization, $F_2^{D(3)}(x_{\mathbf{P}}, \beta, Q^2) = f_{\mathbf{P}}(x_{\mathbf{P}})F_{2\mathbf{P}}(\beta, Q^2)$, with the process independent flux of pomerons in the proton $f_{\mathbf{P}}(x_{\mathbf{P}})$ and the $x_{\mathbf{P}}$ independent structure function $F_{2\mathbf{P}}(\beta, Q^2)$ **does not exist in QCD**.

Besides this diffractive factorization breaking, we predicted an unprecedented dominance of the higher twist $F_L^{D(3)}$ at $\beta \gtrsim 0.9$, which makes the DGLAP evolution of F_2^D completely invalid at large β . Still further, upon the k^2 integration, the factor $[1 - 2(k^2 + m_f^2)/M^2]$ in (3) transforms into the factor $\sim \left[1 - \frac{m_f^2}{Q^2(1-\beta)}G^2(x_{\mathbf{P}}, \frac{1}{4\beta}Q^2)\right]$ in $F_T^{D(3)}$ [27]. Such an abnormal enhancement of a higher twist, $\propto G^2(x_{\mathbf{P}}, \frac{1}{4\beta}Q^2)$, is unprecedented in DIS. This higher twist is especially large at $\beta \rightarrow 1$ and is a further strong objection to the blind DGLAP evolution of $F_T^{D(3)}$. This higher twist is a likely explanation [27] of the H1 finding [25] of the rise of $F_2^{D(3)}$ with Q^2 even for large β , for the related discussion see also [28]. In the CC DDIS there are still more higher twists which are due to the nonconservation of charged currents [1].

The non-negotiable prediction from pQCD is a substantial intrinsic charm in the pomeron [4,8,10], the abundance of which for $\beta \gtrsim 0.1$ is predicted to rise from $\approx 3\%$ at $x_{\mathbf{P}} = 10^{-2}$ to $\approx 25\%$ at $x_{\mathbf{P}} = 10^{-4}$. We predicted the charm abundance $\sim 15\%$ at $\beta \ll 1$ from excitation of the $c\bar{c}g$ and higher states. This intrinsic charm explains perfectly the diffractive charm data reported at DIS'97 [29,30] without invoking unnatural hard glue in the pomeron.

The above findings did not make their way yet into the widely used Monte Carlo codes for DDIS, which are all still based on the discredited diffractive factorization and the DGLAP evolution of the large- β diffractive structure function. As we have seen above, the transverse momentum structure of final states in DDIS is quite different from that in the standard DIS. An analysis [5] of higher orders in DDIS has shown that the structure of real and virtual radiative corrections in DDIS and standard DIS is different, and one needs more work on final state radiation

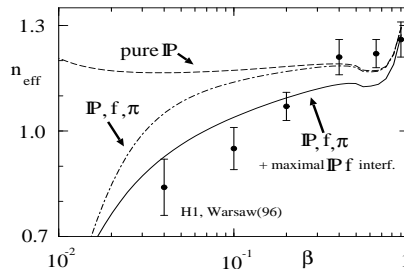


FIGURE 2. The effective exponent n_{eff} in the fit $F_2^{D(3)} \propto x_{\mathbf{P}}^{1-n_{eff}}$ for the pure pomeron contribution to $F_2^{D(3)}$ ([8], dashed curve) and with allowance for the f and π exchange in the weak $f\mathbf{P}$ (dot-dashed curve) and strong $f\mathbf{P}$ interference scenarios [24].

before turning on hadron shower codes which were developed for, and fine tuned to, the standard DIS final states. In conclusion, all the DGLAP analysis and the factorization model-based conclusions on the hard glue in the pomeron are suspect. One badly needs Monte-Carlo implementation of the color dipole picture with due incorporation of the above host of pQCD scales, which is not available at the moment.

The situation changes at $\beta \ll 1$, where $F_2^{D(3)}(x_{\mathbf{P}}, \beta, Q^2)$ has been proven to satisfy the conventional DGLAP evolution in β, Q^2 (at least for a fixed $x_{\mathbf{P}}$) [5]. The obvious conclusions are the rise of $F_2^{D(3)}(x_{\mathbf{P}}, \beta, Q^2)$ as β decreases and/or Q^2 rises and (still approximate) applicability of the conventional parton model for hard scattering off the pomeron.

Incidentally, via unitarity the diffractive higher twist also implies substantial higher twist effects in the proton structure function at $x \ll 1$, which hitherto has been ignored in the QCD analysis of the HERA data.

TRIPLE-REGGE REVISITED

The real reason behind the plethora of pQCD scales and effective intercepts $\alpha_{\mathbf{P}}$ which vary with $Q^2, \beta, x_{\mathbf{P}}$ and flavor, is that the QCD pomeron described by the running BFKL equation is a sequence of **moving** poles with intercepts $\Delta_n = \Delta_{\mathbf{P}}/(n+1)$ [31–33]. Here n labels the eigenfunctions $\sigma_n(r)$ of the running BFKL equation for the dipole cross section and equals the number of nodes in $\sigma_n(r)$, for more details see Zoller’s talk at DIS’97 [33]. The onset of the dominance of the rightmost pole with $\alpha_{\mathbf{P}} = 1 + \Delta_{\mathbf{P}}$ is elusive because of the substantial contribution from the subleading poles in the range of x accessible at HERA [34,32].

Besides the subleading pomeron poles, DDIS at a moderately small $x_{\mathbf{P}}$ picks secondary reggeon exchanges (f, π). The f exchange in the γ^*p scattering originates from DIS off the valence quarks and is represented by color singlet $q\bar{q}$ exchange in the t -channel. Because of the kinematical relation, $x_{\mathbf{P}} = x/\beta$, the f -reggeon exchange is most prominent in DDIS at small β and lowers the exponent n_{eff} in

the fit $F_2^D \propto x_{\mathbf{P}}^{1-n_{eff}}$, which is evident in the discussion of the proton spectra in [35] and has indeed been observed by the H1 [25].

Eventually, one must be able to relate the f -exchange in DDIS to the valence structure function of the proton and to calculate the structure function of the reggeon directly from pQCD [36]. The existing triple-Regge analyses [25,24,37] rather use the model estimates for the flux of reggeons from hadronic diffraction and take for the reggeon the pion structure function. The major issue is the reggeon-pomeron interference. If one treats the pomeron and reggeon as "orthogonal hadronic states", then the interference must be weak [24]. To the contrary, the pQCD suggests [36] a strong constructive reggeon-pomeron interference. The strong interference scenario is preferred by the H1 data shown in Fig. 2.

FORWARD DIFFRACTION CONE IN DDIS

The p_{\perp}^2 dependence of diffractive cross section is a new observable accessible with the advent of the LPS era. The standard parameterization is $d\sigma^D \propto \exp(-B_d p_{\perp}^2)$. The so-defined diffraction slope B_d is a fundamental measure of the interaction radius. For the two-body scattering $ac \rightarrow bd$, an essentially model-independent decomposition is $B_d = \Delta B_{ab} + \Delta B_{cd} + \Delta B_{int}$, where ΔB_{ij} come from the size of the ij transition vertex and ΔB_{int} comes from the interaction range proper. The values of ΔB_{ij} depend strongly on the excitation energy in the $i \rightarrow j$ transition. The situation in hadronic diffraction can be summarized as follows ([38], see also the review [39]): In the elastic case, $i = j$, and for excitation of resonances and of the low-mass continuum states, $\Delta m \lesssim m_N$, which fall into the broad category of *exclusive* diffraction, one finds $\Delta B_{ij} \sim \Delta B_{ii} \approx \frac{1}{3}R_i^2$ and $B_d \sim B_{el}$. Here R_i^2 is the hadronic radius squared. In the hadronic elastic scattering $\Delta B_{ii} \sim 4-6 \text{ GeV}^{-2}$, and typically $B_{el} \sim 10 \text{ GeV}^{-2}$. But if $\Delta m \gtrsim m_N$, i.e., then $\Delta B_{ij} \sim 0$. For instance, only the target proton size, and ΔB_{int} , contribute to B_d in the triple-pomeron region of truly *inclusive* diffraction $hp \rightarrow Xp'$ summed over all large-mass diffractive states, $M^2 \gtrsim (5-10) \text{ GeV}^2$. Here one finds $B_d = B_{3\mathbf{P}} = \Delta B_{pp} + \Delta B_{int} \sim \frac{1}{2}B_{el} \approx 6 \text{ GeV}^{-2}$. In the double high-mass diffraction $hp \rightarrow XY$, when $M_{X,Y} \gg m_N$, one is left with $B_d \sim \Delta B_{int} \sim 1.5-2 \text{ GeV}^{-2}$ (for the especially illuminating data on double diffraction see [40]). The Regge shrinkage of the diffraction, i.e., the Regge rise of B_{el} with energy, was seen in all elastic scattering processes; there is as yet no clear evidence for the shrinkage of the diffraction cone for diffraction dissociation.

The remarkable feature of $B_{3\mathbf{P}}$ is its universality, because the dependence on the diffracting beam and diffractively produced state drops out; the same $B_{3\mathbf{P}} \sim 6 \text{ GeV}^{-2}$ is found for $h = p, \pi, K$ and for real photoproduction $\gamma p \rightarrow Xp'$ [41]. Furthermore, the absence of the Q^2 dependence and the same $B_d \approx B_{3\mathbf{P}}$ has been argued to hold for DDIS at $M^2 \gg Q^2$, i.e., at $\beta \ll 1$ [4], which agrees with the first data from ZEUS LPS: $B_d = 7.1 \pm 1.1_{-1.0}^{+0.7} \text{ GeV}^{-2}$ in DDIS for $5 \text{ GeV}^{-2} < Q^2 < 20 \text{ GeV}^{-2}$ [22] and $B_d = 7.7 \pm 0.9 \pm 1.0 \text{ GeV}^{-2}$ in real photoproduction [42].

DDIS at moderate and large β is the tricky one. Here the principal issues are: i)

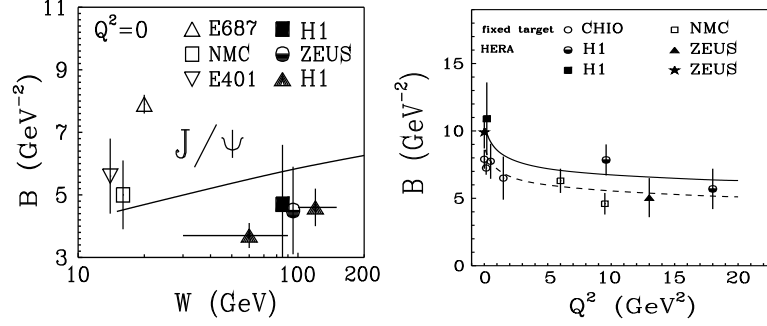


FIGURE 3. Predictions from the color dipole approach for diffraction slope [44] vs. the experimental data. The left box: the Regge growth of the diffraction slope for real photoproduction of the J/Ψ . The right box: the Q^2 dependence of the diffraction slope for the ρ^0 production.

what is the typical dipole size (scanning radius) in the γ^*X transition, and ii) where is the borderline between *exclusive* and *inclusive* DDIS, *i.e.*, what is the relevant excitation scale - the hadronic scale Δm or $\sqrt{Q^2}$?

We start with extreme case of exclusive diffraction: elastic production of vector mesons $\gamma^*p \rightarrow Vp$. The major predictions from the color dipole dynamics for elastic production are [43,44]: i) The QCD pomeron is a series of **moving** poles, the Regge shrinkage persists at all Q^2 and for all vector mesons we predict the rise of B_d by $\sim 1.5 \text{ GeV}^{-2}$ from the CERN/FNAL to HERA energy (Fig. 3). ii) Because of the shrinkage of the photon and the decrease of the scanning radius r_S with Q^2 , we predict $\Delta B_{\gamma^*V} \propto r_S^2 \propto 1/(Q^2 + m_V^2)$, in agreement with the experiment, see Fig. 3 (a more detailed analysis reveals a nontrivial slowly decreasing contribution to ΔB_{γ^*V} which, however, is numerically small: $\Delta B_{\gamma^*V} \sim R_c^2/G(x, \tau(Q^2 + m_V^2))$ [44]). iii) In the proton dissociative vector meson production one expects [38] $B_d \sim B_{int}$ plus a contribution from the γ^*V transition vertex which is small at large Q^2 , which has been confirmed experimentally. For instance, H1 found $B_d = 2.1 \pm 0.5 \pm 0.5$ for the proton dissociative electroproduction of the ρ^0 at $Q^2 > 7 \text{ GeV}^{-2}$ [45] and $B_D = 1.8 \pm 0.3 \pm 0.1 \text{ GeV}^{-2}$ [46]. iv) Restoration of flavor symmetry is predicted, *i.e.*, the values of B_D for different vector mesons must be to a good accuracy equal if production of different vector mesons is compared at equal $Q^2 + m_V^2$.

Evidently, in the elastic production $B_d \gtrsim \Delta B_N \sim (4-6) \text{ GeV}^{-2}$. The HERA results give much too small $B_d(\gamma^* \rightarrow J/\Psi)$. A likely explanation is an admixture of proton diffractive $\gamma^*p \rightarrow J/\Psi + Y$, in which $B_d = \Delta B_{int} \sim 1.5-2 \text{ GeV}^{-2}$. The LPS data can clarify the situation. If an anomalously small values of $B_d(\gamma^* \rightarrow J/\Psi)$ will persist, it will mean we don't understand the size of protons as probed by gluons and will put in trouble many a models of diffractive production.

Because of the node in the radial wave function of radially excited $V'(2S)$, diffractive production $\gamma^*p \rightarrow V'(2S)p'$ is predicted to have many peculiarities: i) strong suppression of the $V(1S)/V'(2S)$ production ratio [16,17,21], which has been well confirmed experimentally, ii) a counterintuitive $B_d(\gamma^* \rightarrow V'(2S)) < B_d(\gamma^* \rightarrow V(1S))$, although $V'(2S)$ has a larger radius, $R(2S) \sim 2R(1S)$ [44]. For instance,

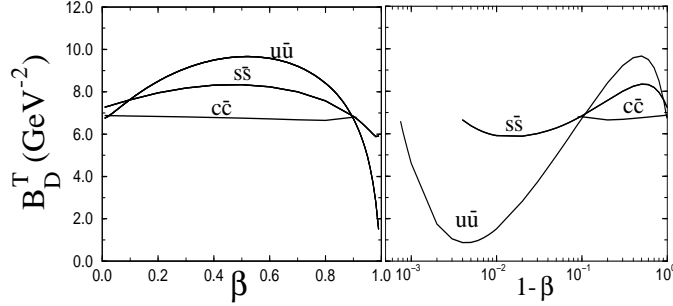


FIGURE 4. Predictions for the diffraction slope for $\sigma_T^{(3)}$ vs. β [47].

for the $\rho'(2S)$ production even the forward dip is possible! These predictions can be tested soon at HERA.

DDIS at finite β is excitation of continuum states, $M^2 = Q^2(1 - \beta)/\beta \gg m_V^2$. If excitation of any continuum were an *inclusive* diffraction, then one could have expected $B_d \approx B_{3\mathbf{P}}$, as in the large-mass hadronic diffraction and/or large-mass real photoproduction. This is not the case in DDIS; careful analysis of the $q\bar{q}$ excitation revealed [47] nontrivial variation of B_d^T about $B_{3\mathbf{P}}$, shown in Fig. 4. First, the excitation scale is set by $\sqrt{Q^2}$ rather than the quarkonium mass, so that the diffraction slope at fixed β must not depend on Q^2 . Second, for $\beta \rightarrow 0$ one indeed finds an approximately flavor independent $B_d^T(\beta \ll 1) \approx B_{3\mathbf{P}}$, whereas for light flavors $B_d^T(\beta \sim 0.5)$ is large, similar to the real photoproduction value of $B(\gamma \rightarrow \rho, \phi)$, as it has been anticipated in [5,8]. Third, for heavy flavors the β -dependence is weaker, because the effective dipole size in the $\gamma^* \rightarrow X$ vertex is smaller: $r^2 \sim (1 - \beta)/m_f^2$. Fourth, the decrease of r^2 with β explains the decrease of $B_d(\beta)$ at $\beta \rightarrow 1$.

The predictions [47] for $\beta \rightarrow 1$, shown in Fig. 4, are extremely interesting from the point of view of the exclusive-inclusive duality [11]. This is a legitimate pQCD region, although a better treatment of the final state $q\bar{q}$ interaction is called. In the extreme limit of $\beta \rightarrow 1$, *i.e.*, $M \sim 2m_f \sim m_V$, the relevant dipole size is given by a small scanning radius r_S and we predict $B_d^T \approx B_d(\gamma^* \rightarrow V)$. At $1 - \beta \sim m_V^2/Q^2$ we predict a substantial drop of the diffraction slope. The drop is $\propto 1/m_f^2$ and comes from the rise of the quark helicity changing $\gamma^* \rightarrow X$ transition with the momentum transfer. The dropping B_d nicely correlates with the prediction [44] of a small diffraction slope for $V'(2S)$ production. To test this prediction, it is necessary to experimentally separate the σ_L from σ_T contributions. Otherwise the observed cross section is dominated by $\sigma_L^{D(3)}$ for which $B_d^L \approx B_{3\mathbf{P}}$, which is uninteresting. These predictions can be tested soon with the LPS data from ZEUS and H1.

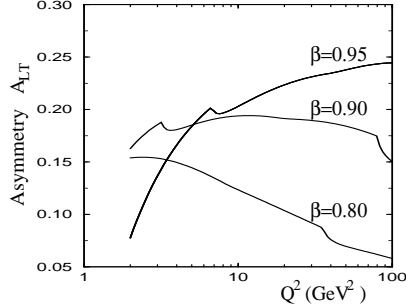


FIGURE 5. Predictions for the (e, e') plane - recoil proton azimuthal asymmetry [47] The spikes on curves are due to flavor thresholds at $Q^2 = 4m_f^2\beta/(1 - \beta)$. .

L/T SEPARATION IN DDIS

Testing the fundamental pQCD prediction [11] of the dominance of $\sigma_L^{D(3)}$ at large β is crucial for the QCD interpretation of DDIS. The measurement of σ_{LT} with LPS is a good substitute for the measurement of $R = \sigma_L/\sigma_T$ by varying the beam energies, which is not possible at the moment. The key is the determination of the quark helicity changing and conserving amplitudes Φ_1 and Φ_2 [4]. They both contribute to $d\sigma_T^{D(3)}$, whereas $d\sigma_L^{D(3)} \sim \frac{1}{Q^2}\Phi_2^2$ and $d\sigma_{LT}^{D(3)} \propto \frac{v_\perp}{Q}\Phi_1\Phi_2$. The azimuthal $\cos\phi$ asymmetry is proportional to $A_{LT} = d\sigma_{LT}^{D(3)}/(d\sigma_T^{D(3)} + d\sigma_L^{D(3)})$. It provides a stringent test of the pQCD mechanism of DDIS. In Fig. 5 we show the pQCD Born approximation for A_{LT} at $x_{\mathbf{P}} \sim 10^{-2}$ and $p_\perp^2 = 0.25 \text{ GeV}^2$; the higher orders do not change the gross features of A_{LT} [47]. For the σ_T -dominated region of $\beta < 0.85$ -0.9, the asymmetry A_{LT} decreases with Q^2 . In contrast, it rises with Q^2 for the σ_L -dominated $\beta > 0.9$. The predicted asymmetry is quite large and is measurable with LPS.

Azimuthal asymmetries for $q\bar{q}$ dijet production offer more tests of the mechanism of DDIS. One interesting prediction [47] is a dependence of B_d^T on the angle ψ between the $q\bar{q}$ plane and \vec{p}_\perp : $B_d^T(\psi) \approx B_d(1 + \delta_T \cos 2\psi)$. For light flavors we predict quite a substantial asymmetry, $\delta_T \sim 0.3$, with a nontrivial β dependence which is different for σ_L and σ_T . For heavy flavors δ_T is smaller. The β and flavor dependence of $\delta_{T,L}$ can be tested even without identification of dijets. It is sufficient to study the azimuthal correlation between the recoil protons and any secondary hadron in the γ^* debris.

The azimuthal correlation between the (e, e') plane and the $q\bar{q}$ dijet plane comes from the $d\sigma_{TT'}$ term in (1). The sign of the $\cos 2\phi$ term is opposite to that for the photon-gluon fusion-dominated jet production in the standard DIS, which is an important signature of the QCD mechanism of DDIS [48].

CONCLUSIONS

The pQCD mechanism of DDIS is well understood. New breakthroughs are expected with the forthcoming LPS data. Fundamental predictions for the diffraction slope, azimuthal asymmetries and σ_L can be tested. Abnormally large higher twist effects, a vast variety of pQCD scales, the resulting breaking of diffractive factorization and inapplicability of the DGLAP evolution to diffractive structure functions have been firmly established theoretically. These findings did not make their way yet into Monte Carlo codes, which are still based on the discredited factorization approximation. Furthermore, final state radiation in DDIS and standard DIS is different and conclusions from Monte Carlo comparisons can be quite misleading. The principal remaining task is a derivation of the real and virtual radiative corrections to DDIS at moderate and large β . We hope to hear more on that at DIS'98 in Brussels.

It is a pleasure to thank the organizers of DIS'97 for an exciting meeting. NNN is grateful to Danny Krakauer for helpful comments on the manuscript.

REFERENCES

1. Bertini M., M.Genovese, N.N.Nikolaev and B.G.Zakharov, paper in preparation.
2. ZEUS: M.Derrick et al. *Z. Phys.* **C68**, 569 (1995)
3. Nikolaev N.N. and B.G. Zakharov, *Z. Phys.* **C49**, 607 (1991)
4. Nikolaev N.N. and B.G. Zakharov, *Z. Phys.* **C53**, 331 (1992).
5. Nikolaev N.N. and B.G.Zakharov, *JETP* **78**, 598 (1994); *Z. Phys.* **C64** (1994) 631.
6. Nikolaev N.N. and B.G.Zakharov, *Phys. Lett.* **B332**, 184 (1996).
7. Nikolaev N.N. and B.G.Zakharov, *Phys. Lett.* **B332**, 177 (1994).
8. Genovese M., N.Nikolaev and B.Zakharov, *JETP* **81** 625 (1995).
9. Genovese M., N.Nikolaev and B.Zakharov, *JETP* **81**, 633 (1995).
10. Genovese M., N.Nikolaev and B.Zakharov, *Phys. Lett.* **B378**, 347 (1996).
11. Genovese M., N.Nikolaev and B.Zakharov, *Phys.Lett.* **B280**, 213 (1996).
12. Bartels J., et al., *Phys. Lett.* **B379**, 239 (1996); E.M.Levin et al., hep-ph/9606280.
13. Buchmuller W., these proceedings. A.Hebecker, these proceedings.
14. Bjorken J.D., and J.B. Kogut, *Phys. Rev* **D8**, 1341 (1973).
15. Nikolaev N.N. and B.G.Zakharov. DIS'96: Deep Inelastic Scattering and Related Phenomena, Editors G.D'Agostini and A.Nigro, World Scientific, Singapore, pp.347-353.
16. Kopeliovich B.Z. and B.G.Zakharov, *Phys. Rev.* **D44** , 3466 (1991).
17. Kopeliovich B.Z., J.Nemchik, N.N.Nikolaev and B.G.Zakharov, *Phys. Lett.* **B309** (1993) 179.
18. B.Z.Kopeliovich, J.Nemchik, N.N.Nikolaev and B.G.Zakharov, *Phys. Lett.* **B324**, 469 (1994).
19. Nemchik J., N.N.Nikolaev and B.G.Zakharov, *Phys. Lett.* **B341** 228 (1994).
20. Nemchik J. et al., *Phys. Lett.* **B374**, 199 (1996).

21. J.Nemchik, N.N.Nikolaev, E.Predazzi and B.G.Zakharov, *INFN preprint DFTT 71/95* (1995) Torino, to be published in *Z.Phys. C*.
22. ZEUS: M.Grothe, these proceedings.
23. Barone V. et al., *Phys. Lett. B292*, 181 (1992).
24. Nikolaev N.N., W.Schäfer and B.G.Zakharov, hep-ph/9608338.
25. H1: M.Dirkmann, this conference
26. Berera A. and D.Soper, *Phys. Rev. D53*, 6162 (1996).
27. Bertini M., M.Genovese, N.N.Nikolaev and B.G.Zakharov, work in progress.
28. Wusthoff M., these proceedings.
29. ZEUS: J.Terron, these proceedings.
30. H1: C.M.Cormack, these proceedings.
31. Lipatov L.N., *Sov. Phys. JETP 63*, 904 (1986).
32. Nikolaev N.N., B.G.Zakharov and V.R.Zoller, *JETP Lett. 60*, 694 (1994). Nikolaev N.N., V.R.Zoller and B.G.Zakharov, paper in preparation.
33. V.R.Zoller, these proceedings.
34. Nikolaev N.N. and B.G.Zakharov, *Phys. Lett. B327*, 149 (1994); **B327**, 157 (1994).
35. Holtmann H. et al., *Phys. Lett. B338*, 363 (1994).
36. Nikolaev N.N., W.Schäfer and B.G.Zakharov, paper in preparation.
37. Golec-Biernat K., J.Kwiecinski and A.Szczurek, hep-ph/9701254.
38. Holtmann H. et al., *Z. Phys. C69*, 297 (1996).
39. Alberi G. and G.Goggi, *Phys. Rep. 74*, 1 (1981).
40. Conta C. et al., *Nucl. Phys. B175*, 97 (1980).
41. Chapin T. et al., *Phys. Rev. D31*, 17 (1985).
42. ZEUS: G.Briskin, these proceedings.
43. Nikolaev N.N., B.G.Zakharov and V.R.Zoller, *Phys. Lett. B366* (1996) 337
44. Nemchik J. et al. paper in preparation
45. H1: C.Adloff et al., **DESY 97-082** (1997).
46. H1: S.Aid et al., *Nucl. Phys. B472*, 3 (1996).
47. Nikolaev N.N., A.Pronyaev and B.G.Zakharov, paper in preparation.
48. Bartels J. et al., *Phys. Lett. B386*, 389 (1996).